J Syst Sci Complex (2012) 25: 71–89

SYNCHRONIZED PATH FOLLOWING CONTROL OF MULTIPLE HOMOGENOUS UNDERACTUATED AUVS*

Xianbo XIANG · Chao LIU · Lionel LAPIERRE · Bruno JOUVENCEL

DOI: 10.1007/s11424-012-0109-2
Received: 11 May 2010 / Revised: 10 January 2011

Abstract This paper addresses the problem of synchronized path following of multiple homogenous underactuated autonomous underwater vehicles (AUVs). The dedicated control laws are categorized into two envelopes: One is steering individual underwater vehicle to track along predefined path, and the other is ensuring tracked paths of multiple vehicles to be synchronized, by means of decentralized speed adaption under the constraints of multi-vehicle communication topology. With these two tasks formulation, geometric path following is built on Lyapunov theory and backstepping techniques, while injecting helmsman behavior into classic individual path following control. Synchronization of path parameters are reached by using a mixture of tools from linear algebra, graph theory and nonlinear control theory. A simple but effective control design on direct inter-vehicle speed adaption with minimized communication variables, enables the multi-AUV systems to be synchronized and stabilized into an invariant manifold, and all speeds converge to desired assignments as a byproduct. Simulation results illustrate the performance of the synchronized path following control laws proposed.

Key words Path following, synchronization, underactuated AUVs.

1 Introduction

Recently, there has been much research activity focusing on coordinated control of multiple autonomous vehicles. Applications of multi-vehicle systems cover the whole world, in space, in the air, on land and at sea. Examples include satellite, spacecraft and aircraft formation flying control[1−2], cooperative control of mobile robots[3−4], coordinated control of marine (surface and underwater) vehicles[5−6], and even the whole collaboration for land, air, sea, and space vehicles[7]. Apparently, multiple vehicles in one team outperform the single vehicle for solo mission in effectiveness and efficiency. Multi-vehicle systems enable enhanced and

Xianbo XIANG
School of Naval Architecture and Ocean Engineering, Huazhong University of Science and Technology, Wuhan 430074*, China; Department of Robotics, LIRMM-CNRS-UMII, UMR* 5506, 161 *rue Ada, Montpellier Cedex* 534095, *France.* Email: Xb.Xiang@lirmm.fr.
Chao LIU · Lionel LAPIERRE · Bruno JOUVENCEL
Department of Robotics, LIRMM-CNRS, UMR 5506, 161 *rue Ada, Montpellier Cedex* 534095, *France.*
*This research was partially supported by the EU FP6 FreeSubNet project under Grant No. 036186, the National Science Foundation of China under Grant No. 51079061, and the Key Laboratory of Education Ministry for Image Processing and Intelligent Control, Huazhong University of Science and Technology under Grant No. 200804. The first author was supported by the European Marie Curie Fellowship.
◇ *This paper was recommended for publication by Editor Yiguang HONG.*

advanced operation through coordinated and cooperative teamwork in civilian, industrial and military fields, such as space-based interferometers, intelligent surveillance and reconnaissance (ISR), patrolling in hazardous environment, undersea oil pipeline inspection, and even hi-tech unmanned combat.

One typical coordinated scenario of multiple underwater vehicles can be envisioned: A fleet of underactuated AUVs is required to get fast acoustic coverage of the seabed. In this valuable mission, vehicles are requested to fly above the seabed at the same depths along parallel paths, and map the seabed using the same suites of acoustic sensors, for examples, side-scan sonar and sub-bottom profile. While traversing parallel paths in the manner of synchronization as a whole, multiple AUVs are able to build the acoustic 3D coverage overlap along the seabed, such that large areas can be completely covered in a short time.

Nevertheless, control design on multi-AUV systems poses significant theoretical challenges. In particular, in the case of underactuated autonomous underwater vehicles (AUVs) there are no actuators in the sway directions, which configuration is by far the most common among marine vehicles. The control problem are far more challenging due to the fact that the motion of underactuated AUVs possesses more degree of freedom (DOF) to be controlled than the number of the independent control inputs under some non-integrable second-order nonholonomic constraints[8−9]. Moreover, the underactuated AUV system is not transformable into a driftless chain system. Consequently, existing control schemes[10−11] developed for chained systems cannot be directly applied to individual underactuated AUV. On the other hand, due to severe underwater acoustic communication constraints in bandwidth[12−13], coordinated control on a fleet of underactuated AUVs keeping synchronized path following with minimized communication is of special interest in practical implementations. That means, besides of developing well-done individual path following controller for each vehicle, the counterpart strategy addressing the synchronization problem is that: The coordinated controllers dealing with inter-vehicle speed adaptation to keep the synchronization behavior, should be decentralized. At the same time, the amount of information exchanged between any two vehicles to fulfill the global control requirements is minimized to one single variable, which is the curvilinear abscissa s_i parameterizing the ith path proposed in this paper.

As pointed out in [14] and [15], a leader-follower type of coordinated path following is adopted. However in [14], it requires a large amount of kinematics and dynamics information, be exchanged between leader and follower, besides complex computation of trajectory tracking controllers as a complement of path following controller. In [15], an important idea of decoupling the spatial assignment (predefined path) and temporal assignment (desired speed) is proposed. The nonlinear feedback law yields convergence of the two vehicles to the respective paths, and forces the follower to accurately track the leader asymptotically. Moreover, only the path parameter of the leader is required to be sent to the follower, which presents a minimum load in the communication network. Unfortunately, this approach cannot be easily generalized to more than two vehicles. The inherent centralized characteristic of the leader-follower control system is vulnerable by single-point failure. The performance of coordination under leader-follower framework suffers from degradation, i.e., any follower who cannot keep up with the leader will fail out of the group, and the whole group will collapse if the leader fails.

A natural way for coordinated control of multiple vehicles is to built a leaderless strategy, and all vehicles have the same priority to reach the coordinated task, which means the strategy of decentralized control for coordinating multiple vehicles is preferred to centralized control scheme. This kind of coordination scheme also exhibits robustness against vehicle failures. In addition, communication signals required in decentralized system are significantly reduced compared with those in centralized control system, as discussed in large-scale control systems for platoons of autonomous underwater vehicles in [16] and references therein. Consequently,

decentralized control is much more applicable for real-world communication situation, especially in underwater acoustic network, since communication bandwidth are severely constrained.

Furthermore, information flow among vehicles in the communication network must be carefully treated, which plays a key role in decentralized control of multiple autonomous system, including multiple virtual agents or physical vehicles. In [17–18], graph is introduced to represent communication network, where each vehicle is one node and each communication link is one edge in the graph. Subsequently, algebraic graph theory supports a rigid methodology to explicitly interpret the relationship between information flow and stability of the cooperating behavior of multiple autonomous system. In the case of multi-agent system, swarming of multiple agents interacting via time-dependent communication links was considered in [19]; In [20], information consensus under dynamically changing interaction topologies was addressed. In [21], both free and constrained flocking with proximity graph representation were provided with respect to classic Reynolds rules in [22], and nearest neighbor rule is used to study the agreement problem of heading aligning in [23]. Hopefully, the elegant technique sheds some light onto the problem of synchronized path following control of multi-AUV systems . In this guidance, local convergence has been resulted by resorting to feedback linearization approach to stabilize a team of wheeled robots[24]. The global performance has been obtained for fully actuated underwater vehicles and tracking error dynamics derived from path parameter is the root to design the coordinated controllers in [25].

In the leading methods reviewed above for coordinated path following control of multiple vehicles, there is a consensus behind the different control techniques in [26] and in [27], that is, individual path following control and inter-vehicle coordination are decoupled, so that the essence of coordinating task is synchronizing suitable state variable to keep the paths following behavior synchronized. Furthermore, paths can be parameterized by the curvilinear along path length, which means synchronization can be achieved by directly adjusting the speed of each vehicles along the path. Therefore, a direct way by regulating speeds of vehicles is proposed. Intuitively, this straightforward mechanism is able to simplify the solution, which inspiring the simple but effective control design in this paper. The decentralized control laws on inter-vehicle speed adaption with minimum communicated variables (i.e., path parameters), enables multi-AUV systems without all-to-all communications, to be synchronized and stabilized into an invariant manifold. Moreover, all speeds converge to desired assignments upon synchronization.

This paper is organized as follows. Section 2 introduces non-singular path following for individual vehicle, with theoretical improvement by injecting helmsman-like behavior as a heading guidance reference. Another important contribution, however, is summarized in Section 3, where a decentralized direct speed adaptation under communication constraints, is derived for synchronized path following of multiple homogenous underactuated AUVs. In Section 4, the performance of the control system proposed is illustrated in simulation results. Finally, Section 5 draws the conclusions and describes some problems that warrant further research.

2 Individual Path Following

This section describes a sharped solution to the problem of path following control for one individual underactuated AUV, where a Helmsman-like behavior is injected into the line-of-sight (LOS) heading guidance. This meaningful behavior embedded in nonlinear controller design, is instrumental to render the tracking error vector exponentially converging to zero.

Normally, there are three basic motion tasks as follows: Point-to-point stabilization, trajectory tracking and path following[27]. Point stabilization covers situations of homing and dynamic positioning of underwater vehicles. The objective of trajectory tracking is to force an

autonomous vehicle to track a stringent time parameterized spatial reference. Path following, is defined as a control problem of driving an autonomous vehicle to follow a specified path at a desired forward speed, which is more suitable for practical undersea implementation, compared with high dependence on the reference model and tightly time constrained control laws of trajectory tracking approach.

The problem of path following was firstly addressed in [28] for kinematic model of wheeled mobile robot. Based on the Serret-Frenet frame $\{F\}$, tracking error vector between vehicle and the tracked path is formulated. The origin of $\{F\}$ is the orthogonal projection of vehicle onto the path, which has an inborn talent to simplify the representation of cross-track error (i.e., closest lateral distance between vehicle and path) as the along-track error is zero. However, it creates a singularity when the robot is located at the center of the path curvature such that the projection point is not uniquely defined. Consequently, only a local convergence of error vector is guaranteed. In order to bypass the singularity, a virtual target moving along the the path is introduced in [29]. Unfortunately, not only the speed of the virtual target but also that of vehicle, have to be adjusted. This disobeys the natural maneuvering specification, when the vehicle is driven to follow the path on the road, the wise driver prefer adjusting the orientation of steering wheel to simultaneously changing the speed of vehicle. In [27], the solution of global convergence was obtained by only steering the rotational angle, with the help of one extra control freedom to dexterously manipulate the speed of virtual target. In this paper, this kind of individual path following design will be stretched, and an implicit Helmsman-like behavior as a heading guidance will be highlighted here. Meanwhile, this method has been successfully extended from kinematics to dynamics via backstepping technique.

2.1 Kinematics and Dynamics Model of Underactuated AUVs

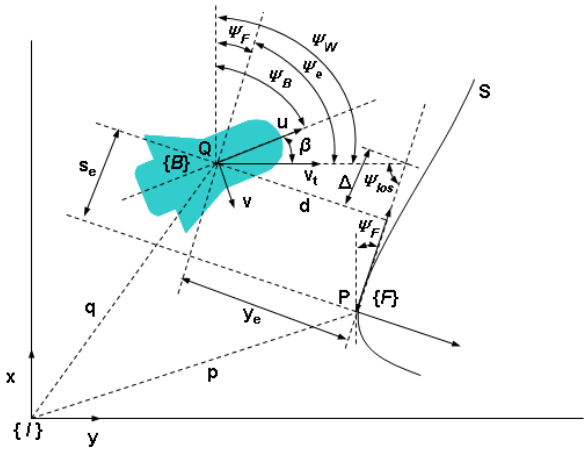

Figure 1 Frame definition and description of problem posed

Each underactuated AUV in the fleet considered in this paper, is equipped with two identical stern thrusters, mounted symmetrically with respect to its longitudinal axis. Recruiting two different kinds of working mode of the thrusters, i.e., common and differential outputs, a force F along the vehicle's longitudinal axis and a torque Γ on its vertical axis are generated, respectively. As there is no lateral thruster, the vehicle is underactuated.

As depicted in Figure 1, let u and v be the longitudinal (surge) and transverse (sway)

velocities, respectively. Let r be the angular speed (yaw rate). Considering the flow frame $\{W\}$ that is obtained by rotating body frame $\{B\}$ around the z_B axis through the sideslip angle β (angle between the surge velocity and the total velocity), the kinematic equations of the AUV can be written as

$$\begin{cases} \dot{x} = v_t \cos\psi_W, \\ \dot{y} = v_t \sin\psi_W, \\ \dot{\psi}_W = r + \dot{\beta}, \end{cases} \tag{1}$$

where $r = \dot{\psi}_B$, and v_t is the total speed of the AUV expressed in $\{W\}$. Clearly, $v_t = \sqrt{u^2 + v^2}$. The control of an AUV system implies considering a permanent positive speed $v_t > 0$ and $v < u$. Then, the sideslip angle β can be defined as $\arctan(v/u)$.

While an underactuated AUV is following a predefined spatial path, P is an arbitrary point on the path, and Q is the center of mass of the moving vehicle. Associated with P, we consider the corresponding Serret-Frenet frame $\{F\}$, where x-axis and y-axis are the normal and tangent unit vectors to the path at P, respectively. The path S is parameterized by a moving target P on the path, with curvilinear abscissa (along path length) denoted by s. Let (s_e, y_e) denote the coordinates of Q be in $\{F\}$. Let the rotations from $\{I\}$ to $\{F\}$ and $\{I\}$ to $\{B\}$ be denoted by the yaw angles ψ_F and ψ_B, respectively. Further, let $c_c(s)$ and $g_c(s)$ denote the path curvature and its derivative respectively, and then $\psi_F = c_c(s)\dot{s}$. With the denotation of variable $\psi_e = \psi_W - \psi_F$, the error dynamics model of the AUV in the Serret-Frenet frame can be derived as

$$\begin{cases} \dot{s}_e = -\dot{s}(1 - c_c y_e) + v_t \cos\psi_e, \\ \dot{y}_e = -c_c \dot{s} s_e + v_t \sin\psi_e, \\ \dot{\psi}_e = r + \dot{\beta} - c_c \dot{s}, \end{cases} \tag{2}$$

where $\dot{\psi}_W = r + \dot{\beta}$ is employed.

The motion dynamics model of the underactuated AUV is obtained by augmenting (1) with the equations

$$\begin{cases} F = m_u \dot{u} + d_u, \\ 0 = m_v \dot{v} + m_{ur} ur + d_v, \\ \Gamma = m_r \dot{r} + d_r \end{cases} \tag{3}$$

with

$$\begin{aligned} m_u &= m - \dot{X}_{\dot{u}}, \quad d_u = -X_{uv} u^2 - X_{vv} v^2, \\ m_v &= m - Y_{\dot{v}}, \quad d_v = -Y_v uv - Y_{v|v|} v|v|, \\ m_r &= I_z - N_{\dot{r}}, \quad d_r = -N_v uv - N_{v|v|} v|v|, \\ m_u r &= m_Y - r - N_r ur, \end{aligned}$$

where m denotes the system mass, I_z is the moment of inertia w.r.t. the z-axis. X, Y, and Z are hydrodynamic derivatives. F and Γ define the inputs of force and torque that is applied to AUV, respectively. The model of underactuated AUV adopted in this paper, is based on the model of the INFANTE AUV, please refer to [30] for more details. We can clearly see that there is no control input in the second equation in (3) due to the absence of thruster on sway direction in the underactuated AUV system.

With the above notation, the problem of path following for single vehicle can be formulated as below:

Individual Path Following Given a predefined path to be followed by a individual underactuated AUV, and given a desired speed profile $u_d(t) \geq u_{\min} > 0$ for the vehicle speed u, derive a feedback control law for F and Γ to drive s_e, y_e and ψ_e asymptotically to zero.

2.2 Nonlinear Controller Design

The controller design for individual path following, is structured in two steps. Firstly, a dedicated reference angle for heading guidance is defined, which will built on classic LOS design, and a Helmsman-like behavior is capsuled inside. And then, nonlinear controller on Lyapunov theory and backstepping techniques, is designed to drive the AUV onto the path.

2.2.1 Heading Design Under LOS Law with Helmsman Like Behavior

In order to follow a predefined path, the most important thing is to steer the vehicle in the right heading, and the desired speed is of second interest. However, the performance of moving towards the path could be quite different, depending on the situation whether a reasonable heading is chosen and a wise computerized "Helmsman" is onboard.

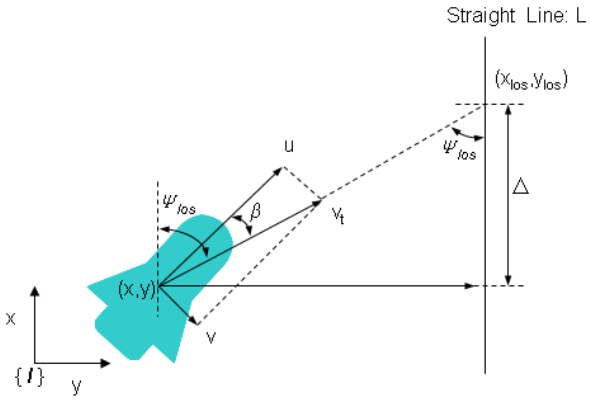

Figure 2 Illustration of the LOS guidance

Classic LOS law for heading guidance is popularly applied in marine surface vehicles[31−32] for tracking straight-line path generated by given way-points during navigation, and this method enlightens us on designing the heading guidance for underwater vehicle to track curved path here.

As depicted in Figure 2, the coordinate origin of the vehicle is (x, y), and the LOS point on the straight-line path is (x_{los}, y_{los}). Thus, the desired yaw angle under LOS guidance is

$$\psi_{los} = \arctan\left(\frac{y_{los} - y}{\Delta}\right).$$

Originally, the control parameter $\Delta(> 0)$ is interpreted as the distance ahead of the ship along the x-axis, i.e., the straight-line path, which the ship should shoot at. The important parameters, look ahead distance Δ, is a constant in LOS design, used to shape the ship moving towards the straight-line path.

Unlike the traditional LOS built in the inertial coordinate, the LOS law built in Serret-Frenet frame is chosen as a heading guidance in this paper, while AUV tracking arbitrary regular path, and the parameter Δ is extended to look at the distance along the tangential path in Serret-Frenet frame as illustrated in Figure 1.

Elaborating more efforts on the heading design, Helmsman-like behavior is introduced. In order to steer a ship towards the straight line, a good Helmsman in [32] will choose the magnitude of heading dependent on the distance from the straight line. In order to follow an arbitrary curvilinear path, a wise Helmsman on board is especially important. When the path has a small

radii of the tangent osculating circle (i.e., large curvature in Serret-Frenet frame) at one point, a good Helmsman is intelligent enough to catch this information, and increase the heading to adhere to the sharp turning path at that moment. On the contrary, the heading guidance decreases when the path is smooth. In this point of view, the LOS angle is adjusted by the Helmsman when the path is not straight, so that Δ is a variable ($\Delta > 0$ and upper bounded). Furthermore, Δ can be a function of curvature $c_c(s)$.

Revisiting Figure 1, in the perfect case of ψ_e equal to the desired heading δ, we can see that $\psi_e = \psi_W - \psi_F$ in the Serret-Frenet frame, is the corresponding LOS angle ψ_{los} described in Figure 2 in the inertial frame. That means the guidance yaw angle can be defined as

$$\delta = \arctan\left(\frac{-y_e}{\Delta}\right), \tag{4}$$

where Δ can be given by

$$\Delta = 2l - lsat(k_0|c_c(s)|), \tag{5}$$

where $0 < k_0 < k_{0\max}$, l is the longitudinal length of the vehicle, and $sat()$ is the saturation function in $(0, 1)$. In the case of straight-line path, Δ could be chosen equal to two vehicle's length, which is corresponding to a standard choice in LOS algorithms.

As in Figure 2, the LOS angle enables the vehicle to turn right ($y_{los} - y > 0$ such that $\psi_{los} > 0$) to follow the straight-line path, when it is on the left side of path, and turn left in the reversal situation. In the situation of arbitrary path as in Figure 1, a wise Helmsman will steer the vehicle onto the tangential path, and command a larger Δ giving a mild approach to the smooth path, while a smaller Δ bringing more aggressive approach to the sharp path. Explicitly, it is convenient for controller in the Serret-Frenet frame to provide the information of curvature, which means the Helmsman behavior can be well embedded in the path following design proposed in this paper.

In a word, the heading reference under LOS law with Helmsman-like behavior illustrated in (4) is physically meaningful, driving the vehicle turn a litter bit sharper in advance where the path curvature will be larger. Moreover, we can see later, it is also instrumental in nonlinear controller design to sharpen the performance of convergence.

2.2.2 Kinematic Controller

As the main objective of the path following control is to drive s_e, y_e an ψ_e to zero, the following Lyapunov function candidate can be considered

$$V_1 = \frac{1}{2}[s_e^2 + y_e^2 + (\psi_e - \delta)^2]. \tag{6}$$

Resorting to the error dynamics model (2), the derivative of V_1 is

$$\dot{V}_1 = -s_e\dot{s} + v_t s_e \cos\psi_e + v_t y_e \sin\psi_e + (\psi_e - \delta)(\dot{\psi}_e - \dot{\delta}).$$

It is straightforward to show that the choice

$$\begin{cases} \dot{s} = k_1 s_e + v_t \cos\psi_e, \\ \dot{\psi}_e = \dot{\delta} - y_e v_t \dfrac{\sin\psi_e - \sin\delta}{\psi_e - \delta} - k_2(\psi_e - \delta), \end{cases} \tag{7}$$

where k_1 and k_2 are positive gains, leads to

$$\dot{V}_1 = -k_1 {s_e}^2 + y_e v_t \sin\delta - k_2(\psi_e - \delta)^2.$$

Replacing the heading reference designed in (4),

$$\dot{V}_1 = -k_1 {s_e}^2 - \frac{v_t {y_e}^2}{\sqrt{{y_e}^2 + \Delta^2}} - k_2(\psi_e - \delta)^2, \tag{8}$$

which means $\dot{V}_1 < 0$ outside the origin.

On the other hand, as the error between the actual orientation and guidance LOS angle is $\dot{\psi}_e = r + \dot{\beta} - c_c \dot{s}$, the yaw rate in kinematics stage can be represented as

$$r = \dot{\delta} - y_e v_t \frac{\sin\psi_e - \sin\delta}{\psi_e - \delta} - k_2(\psi_e - \delta) - \dot{\beta} + c_c \dot{s}. \tag{9}$$

Hence, the kinematic control law can be written as

$$\begin{cases} \dot{s} = k_1 s_e + v_t \cos\psi_e, \\ r = \dot{\delta} - y_e v_t \dfrac{\sin\psi_e - \sin\delta}{\psi_e - \delta} - k_2(\psi_e - \delta) - \dot{\beta} + c_c \dot{s}, \end{cases} \tag{10}$$

where the first equation is the virtual control input $\dot{s}$, which can be considered as a virtual target moving along the path cooperatively adjusts its own speed $\dot{s}$ depending on the projection of the vehicle's speed on the path $v_t \cos\psi_e$ and the along abscissa tracking error s_e, in order to help the AUV converge to the path; the second equation is the control input of yaw rate which changes the orientation of the vehicle according to the heading guidance, such that the vehicle moves towards the predefined path.

2.2.3 Dynamics controller

In the overall control loop, the kinematics controller actually acts as a reference subsystem, giving the desired signals for the control subsystem based on the dynamics level. Using backstepping techniques[33], the control law in kinematic level can be extended to deal with vehicle dynamics.

Let r_d (desired yaw rate) be the reference signal of r (actual yaw rate), which derived from kinematic model. That means the desired yaw rate as a reference for dynamics controller can be written as

$$r_d = \dot{\delta} - y_e v_t \frac{\sin\psi_e - \sin\delta}{\psi_e - \delta} - k_2(\psi_e - \delta) - \dot{\beta} + c_c \dot{s}, \tag{11}$$

where $\delta = \arctan(\frac{-y_e}{2l - lsat(k_0|c_c(s)|)})$, $0 < k_0 < k_{0\max}$.

Then, applying backstepping technique, the difference between the actual yaw rate and the desired yaw rate, which must be reduced to zero. This inspires us to design the Lyapunov candidate function:

$$V_2 = \frac{1}{2}[s_e^2 + y_e^2 + (\psi_e - \delta)^2 + (r - r_d)^2]. \tag{12}$$

With s_e, y_e in error dynamics formulation (2) and $\dot{s} = k_1 s_e + v_t \cos\psi_e$ is given in kinematics control laws (7), the derivative of V_2 is

$$\dot{V}_2 = -k_1 s_e^2 + y_e v_t \sin\delta + (\psi_e - \delta)(\dot{\psi}_e - \dot{\delta}) + (r - r_d)(\dot{r} - \dot{r}_d).$$

Choose

$$\dot{r} = \dot{r}_d - k_3(r - r_d) - (\psi_e - \delta), \tag{13}$$

then

$$\dot{V}_2 = -k_1 s_e^2 + y_e v_t \sin\psi_e + (\psi_e - \delta)[(\dot{\psi}_e - \dot{\delta}) - (r - r_d)] - k_3(r - r_d)^2.$$

As desired yaw rate is a reference signal from kinematic controller given in (11). After tedious calculation, we can get

$$\begin{aligned}\dot{V}_2 =& -k_1 s_e^2 - k_2(\psi_e - \delta)^2 - y_e v_t \sin\psi_{los} - k_3(r - r_d)^2 \\ =& -k_1 s_e^2 - k_2(\psi_e - \delta)^2 - y_e^2 v_t / \sqrt{y_e^2 + \Delta^2} - k_3(r - r_d)^2.\end{aligned} \tag{14}$$

That means $\dot{V}_2 < 0$ other than the origin.

The control laws of virtual input s and input torque Γ are:

$$\begin{cases} \dot{s} = k_1 s_e + v_t cos\psi_e, \\ \Gamma = m_r \dot{r} + d_r = m_r(\dot{r}_d - k_3(r - r_d) - (\psi_e - \delta)) + d_r, \end{cases} \tag{15}$$

where the virtual input has the same physical meaning as describe in (10), which cooperatively adjusts its own speed to help the AUV converge to the path; the second term is the actual control input of torque such that the orientation of the vehicle can be changed towards the tangential direction of the predefined path.

Clearly, the dynamic control law above requires the computation of acceleration $\ddot{\beta}$, which is the second derivative of side slip angle and cannot be measured directly, and one must resort to the dynamic model of the AUV to get it. In the case of a stern dominant vehicle, this computation is well posed. For a bow dominant vehicle, the sign of $m - Y_r$ should be taken into account, please refer to [34] for detailed formulation.

Proposition 1 *Let guidance heading be given by* (4)*, and control law be given by* (15) *for some* $k_i > 0$ $(i = 1, 2, 3)$*. Let* $\min\{k_1, k_2, k_3\} \geq \frac{v_t}{\Delta}$*,* $v \geq v_{t\min} > 0$ *and* $\Delta > 0$ *be guaranteed. Then the equilibrium point* $(s_e, y_e, \psi_e) = 0^3$*, is globally uniformly exponentially stable.*

Proof The Lyapunov function V_2 given by (12) is positive definite and radially unbounded. The derivative of Lyapunov function $\dot{V}_2$ given by (14) is negative definite. Hence, by standard Lyapunov arguments, s_e, y_e, $(r - r_d)$, and $(\psi_e - \delta)$ global uniformly asymptotically converge to 0. With heading guidance (4), δ converges to y_e, and y_e converges to δ, such that ψ_e has the same characteristics with y_e, and also converges to 0 in the end.

If $\min\{k_1, k_2, k_3\} \geq \frac{v_t}{\Delta}$, the derivative of Lyapunov function (14) becomes $\dot{V}_2 \leq -\frac{v_t}{\Delta}[s_e^2 + y_e^2 + (\psi_e - \delta)^2 + (r - r_d)^2] \leq -\frac{2v_t}{\Delta} V_2$ (as $\frac{v_t}{\Delta} \geq \frac{v_t}{\sqrt{{y_e}^2 + \Delta^2}} > 0$), which means Lyapunov function is quadratically negative definite. Hence, by standard Lyapunov arguments, the equilibrium point $(s_e, y_e, \psi_e) = 0^3$, is globally uniformly exponentially stable with convergent rate of $v_t/2\Delta$, when $v_t = k_v\sqrt{y_e^2 + \delta^2}$, $k_v > 0$. ∎

Remark: 1) Singularity is relaxed by the introduction of an extra degree of freedom for control design, which is attached to the virtual target. See [29] in detailed analysis.

2) In [27] and [34], only global asymptotically stable is guaranteed. With helmsman like behavior and LOS guidance embedded in the controller design, the performance of global exponentially convergence derived herein is indeed stronger.

3) Actually, this is a sharp solution to the traditional path following control, both on mathematic level (performance of convergence) and physic level (performance of helmsman like heading).

4) In (15), $\ddot{\beta}$ is requested for control on torque input Γ, but the variable $\ddot{\beta}$ cannot be measured in practice. Moreover, β is not directly controllable for underactuated AUV and cannot converge to a desired side slip angle rigorously, as there is no lateral thruster contributing force to steer sway speed v in an underactuated AUV. It is different from the case of fully

actuated AUV where β is controllable by the surge and sway forces and converges to a desired sideslip angle β_d. Therefore, one must resort to the original dynamic model of the AUV for the computation of $\beta, \dot{\beta}, \ddot{\beta}$.

It is straightforward to get

$$\begin{cases} \beta = \arctan \dfrac{v}{u}, \\ \dot{\beta} = \dfrac{1}{v_t^2}(u\dot{v} - v\dot{u}), \\ \ddot{\beta} = \dfrac{1}{v_t^2}(u\ddot{v} - v\ddot{u}) - 2\dfrac{\dot{v}_t}{v_t}\dot{\beta}, \end{cases} \tag{16}$$

where $\dot{u}$ and $\dot{v}$ can be easily derived from (3). However, the computation of $\ddot{u}$ and $\ddot{v}$ must resort to the dynamics model of the AUV, we can get

$$\begin{cases} \ddot{u} = \dfrac{1}{m_u}(\dot{F} - \dot{d}_u), \\ \ddot{v} = \dfrac{1}{m_v}(-m_{ur}\dot{u}r - m_{ur}u\dot{r} - \dot{d}_v). \end{cases} \tag{17}$$

3 Synchronized Path Following

Before addressing the problem of synchronized path following for multiple underactuated AUVs, the communication topology among vehicles has to be explicitly represented. It is important to derive decentralized controller for a fleet of AUVs under severe underwater acoustic communication constraints. Fortunately, the algebraic graph theory is a useful tool, as each AUV can be taken as a vertex, and each acoustic communication link can be a edge of graph.

3.1 Preliminaries of Algebraic Graph Theory

Now, we review some basic concepts of graph and matrices associated with graph, which are the preliminaries of algebraic graph theory and Laplacian matrix. One can see [35] for more details and the references therein.

An information topology is defined by a graph $G(V, E)$ with N vertices in a set of vertices V, and a set of edges E with edges $e_{ij} = (v_i, v_j) \in E$ and $v_i, v_j \in V$. We say that vertex v_i and v_j are connected if $(v_i, v_j) \in E$, and two vertices on the same edge or two edges with a common vertex are adjacent. If two edges have a common vertex, then they are incident with this vertex. The adjacent matrix A of graph G, is a positive square matrix of size $|V|$, whose ijth element $a_{ij} = 1$ if $(v_i, v_j) \in E$, and is zero otherwise. The degree matrix D of an undirected graph G, is the diagonal matrix with the number of its neighbors of each vertex along the diagonal denoted by $\deg(v_i)$, where the set of neighbors of node i is denoted by $N_i = \{j : (v_i, v_j) \in E\}$. The Laplacian matrix L of an undirected graph is defined as $L = D - A$. A path is a sequence of edges from v_i to v_j, such that two consecutive vertices are adjacent. A graph is said connected if there is a path between any distinct pair of vertices.

The following lemmas are well known in algebraic graph theory[35].

Lemma 1 *The laplacian potential L of a undirected graph is positive semi-define and satisfies the following identity, $X^{\mathrm{T}}LX = \sum\limits_{i,j\in E}(x_i - x_j)^2$, where $X = [x_1, x_2, \cdots, x_n]^{\mathrm{T}}$ is the state vector of vertices.*

Lemma 2 *The Laplacian matrix of a connected graph, only has one single zero eigenvalue and the corresponding eigenvector is the vector of ones,* $\vec{1}$.

Both of them are very important characteristics of Laplacian matrix, and they are instrumental in designing coordinated strategy for synchronized path following controller of multiple underactuated AUVs.

3.2 Synchronized Controller Design for Homogenous AUVs

For homogenous underactuated AUVs with same dynamics, driving u to u_d, but not the total speed v_t to v_{td}, is enough to enable the underactuated AUVs to follow the path with synchronization. In the case of heterogenous underactuated AUVs, all the total speed v_t are required to align with the desired total speed v_{td}, as the dynamics are different from underactuated characteristics, such that the same u_d does not bring the same v_{td} in the case of heterogenous AUVs. Recall that β is not directly controllable for underactuated AUV and cannot converge to a desired side slip angle rigorously, as there is no lateral thruster contributing force to steer sway speed v in an underactuated AUV. In this point of view, we can conclude that v_t converge to v_{td} is necessary for heterogenous vehicles to follow the path with synchronization, and the transformation from u to v_t has to be built and embodied in the dynamics (F and Γ), which far more increase the complexity of control computation. However, driving u to proper u_d, is enough in the coordinated controller for homogenous underactuated AUVs to reach synchronized path following.

Deliberately, the design of control input F in dynamics level, is lagged here. Consider Lyapunov function candidate, $V_u = \frac{1}{2}(u - u_d)^2$. It is trivial to choose the control law $\dot{u} = \dot{u}_d - k_4(u - u_d)$ where $k_4 > 0$, or rather that

$$F = m_u\dot{u} + d_u = m_u(\dot{u}_d - k_4(u - u_d)) + d_u. \tag{18}$$

With (18), control force solely drives the vehicle speed u converge to desired speed u_d assuming $u_d(t) \geq u_{\min} > 0$, with performance of globally uniformly exponentially stable. It indicates that controlling u is totally decoupled with other control behaviors, i.e., driving the vehicle onto the path with s_e, y_e, ψ_e equal to zero is decoupled with driving u_t to u_{td}. This important theoretic root endows the controller with another dedicated ability of speed adaptation among vehicles, without degrading the performance of vehicle's convergence to the path.

Therefore, the feasible strategy for synchronized path following is that:

1) Geometric task: each vehicle will recruit its own path following control law to track the path, such that $(s_e, y_e, \psi_e)^{\mathrm{T}} = (0, 0, 0)^{\mathrm{T}}$.

2) Synchronized task: Adjusting the desired speed of each vehicle, make the synchronizing parameters, tracked curvilinear abscissa (length along the path) $s_i (i = 1, 2, \cdots, n)$ herein, to be equal, such that $s_i = s_j, i \neq j, i, j \in \{1, 2, \cdots, N\}$.

In this paper, it is assumed that, 1) the communications between any pair of vehicle is reciprocal (i.e., bidirectional link) such that L is symmetric, and 2) the communication graph is connected.

With the above notation, the problem of synchronized path following for multiple underactuated vehicles can be formulated as below:

Synchronized Path Following of Homogenous Underactuated AUVs Consider n homogenous underactuated AUVs with kinematic and dynamic models given by (1) and (3), respectively. Given n spatial parallel paths to be followed by AUVs, and a desired profile u_d for the final speed along the paths, derive feedback control laws, so that s_{e_i}, y_{e_i}, ψ_{e_i} ,$u_i - u_{d_i}$, and $s_i - s_j$ tend to zero asymptotically.

The coordinated controller design for synchronized path following of homogenous underactuated AUVs, is derived in three steps as following.

Step 1 Given individual path following control law (15) for each vehicle, the multi-AUV systems uniformly globally exponentially reach the largest invariant set $\{\Omega_{Path}|(s_{e_i}, y_{e_i})^{\mathrm{T}} = 0^2, \psi_{e_i} = 0, i = 1, 2, \cdots, n\}$.

Step 2 Given individual path following control law (18) for each vehicle, the multi-AUV systems uniformly globally exponentially reach the largest invariant set $\{\Omega_u|(s_{e_i}, y_{e_i})^{\mathrm{T}} \in \Re^2, \psi_{e_i} \in \Re, u_i = u_{d_i}, i = 1, 2, \cdots, n\}$.

Step 3 Let's study the trajectories of the vehicles onto the largest invariant set Ω_{Path} and Ω_u. Under these two invariant sets, that is $\{\Omega_{Path} \cap \Omega_u\}$, all vehicles are on their own paths and will move along these paths with desired speeds. That means, each vehicle coincides with the corresponding virtual target moving on the individual path. So, we can claim that $\dot{S} = U_d$ as along as the control laws exist, where the desired speed profile $U_d = [u_{d1}, u_{d2}, \ldots, u_{dn}]^{\mathrm{T}}$, and $S = [s_1, s_2, \ldots, s_n]^{\mathrm{T}}$.

Considering Lyapunov candidate function

$$V_S = \frac{1}{2} S^{\mathrm{T}} L S. \tag{19}$$

As illustrated in Lemma 1, V_S has a quadric form such that $V_S \geq 0$.

With the condition that, there are reciprocal communication links among each pair of nodes, which contributes to symmetric Laplacian matrix $L = L^{\mathrm{T}}$. The time-derivative of V_S is

$$\dot{\mathbf{V}}_{\mathbf{S}} = \frac{1}{2} \dot{S}^{\mathrm{T}} L S + \frac{1}{2} S^{\mathrm{T}} L \dot{S} = S^{\mathrm{T}} L \dot{S}.$$

Let the desired speed profile be

$$\boldsymbol{U_d} = \frac{u_{\max} + u_{\min}}{2} \vec{1} - \left(\frac{u_{\max} - u_{\min}}{2\pi} \right) \cdot \arctan(LS),$$

where $u_{\min} = [u_{1\,\min}, u_{2\,\min}, \cdots, u_{n\,\min}]^{\mathrm{T}}$, and $u_{\max} = [u_{1\,\max}, u_{2\,\max}, \cdots, u_{n\,\max}]^{\mathrm{T}}$. $u_{i\,\min}$ and $u_{i\,\max}$ are the minimum and maxim speed of vehicle i $(i = 1, 2, \cdots, n)$, respectively.

In order to simplify the matrix manipulation, special notations are made as following:

1) $\arctan(LS) = [\arctan(L_1 S), \arctan(L_2 S), \cdots, \arctan(L_n S)]^{\mathrm{T}}$, and $L_i S$ represents the ith row of Laplacian matrix L.

2) $(\frac{u_{\max} - u_{\min}}{2\pi}) \cdot \arctan(LS)$ represents Hadamard product of matrix $(\frac{u_{\max} - u_{\min}}{2\pi})$ and matrix $\arctan(LS)$. For two matrices with the same dimensions, Hadamard product, is also known as the entrywise product and the Schur product, with the definition of $(A \cdot B)_{i,j} = A_{i,j} \cdot B_{i,j}$.

For homogenous AUVs, assuming that

$$\frac{u_{i\,\max} + u_{i\,\min}}{2} = \frac{u_{j\,\max} + u_{j\,\min}}{2} = u_{d0}, \tag{20}$$

where $i \neq j, i, j \in \{1, 2, \cdots, n\}$.

Then,

$$\boldsymbol{U_d} = u_{d0} \vec{1} - \left(\frac{u_{\max} - u_{\min}}{2\pi} \right) \cdot \arctan(LS). \tag{21}$$

Proposition 2 *Consider the communication topology of multi-AUV systems represented by a connected graph with reciprocal links, let individual path following controller be given by* (15) *and* (18)*. Let decentralized speed adaptation be given by* (21) *under the condition of* (20)*. Then*

the homogenous underactuated multi-AUV systems are globally asymptotically synchronized to an invariant manifold $\{\Omega_S|LS=0\}$*, that is,* $s_1=s_2=\cdots=s_n$*. Meanwhile, the speeds of all vehicles globally asymptotically converge to a constant value* $(u_{i\max}+u_{i\min})/2$*.*

Proof As the trajectories of the system onto the invariant set Ω_{Path} and Ω_v, $\dot{S}$ equals to U_d.

$$\begin{aligned}\dot{\boldsymbol{V}}_S &= U_d S^{\mathrm{T}} L\vec{1} - (LS)^{\mathrm{T}}\left(\left(\frac{u_{\max}-u_{\min}}{2\pi}\right)\cdot\arctan(LS)\right)\\ &= -(LS)^{\mathrm{T}}\left(\left(\frac{u_{\max}-u_{\min}}{2\pi}\right)\cdot\arctan(LS)\right).\end{aligned}$$

There are three steps to simplify the derivative of Lyapunov function:

1) Due to the fact that the sum of row vector of L equals to zero, $L\vec{1}=0$, such that $U_d S^{\mathrm{T}} L\vec{1}=0$.

2) $(LS)^{\mathrm{T}}((\frac{u_{\max}-u_{\min}}{2\pi})\cdot\arctan(LS)) = \frac{1}{2\pi}\sum_{i=1}^{n}(u_{i\max}-u_{i\min})(L_iS)\arctan(L_iS)$. As the function $f(x)=(x)\arctan(x)\geq 0$, $(L_iS)\arctan(L_iS)\geq 0$. In addition, $(u_{i\max}-u_{i\min})>0$, such that $(u_{i\max}-u_{i\min})(L_iS)\arctan(L_iS)\geq 0$.

3) As there is $U_d S^{\mathrm{T}} L\vec{1}=0$ in above step 1), and $(u_{i\max}-u_{i\min})(L_iS)\arctan(L_iS)\geq 0$ in step 2), $\dot{V}_S\leq 0$, that is, V_S is a nonnegative and monotonically non-increasing function up to a well-defined limit $\lim_{t\to\infty} V_S = l_1$, which means $V_S = S^{\mathrm{T}}LS$ is bounded.

Moreover, it is straight forward to show that $\ddot{V}_S$ is bounded so that $\dot{V}_S$ is uniformly continuous. Then, using Barbalat's lemma, $\dot{V}_S$ tends to 0 as t tends to ∞, that is $\dot{V}_S = \frac{1}{2\pi}\sum_{i=1}^{n}(u_{i\max}-u_{i\min})(L_iS)\arctan(L_iS)$ tends to 0, which means $(L_iS)\arctan(L_iS)=0$, and $L_iS=0$ at last.

Now, we can conclude that the state of the system converges to the largest invariant subset, i.e., invariant manifold $M=\{S\in\Re^n|LS=0\}$, under decentralized control law (21), and condition of speed (20).

Interestingly, the invariant manifold M implies that, S are eigenvectors of L corresponding to the zero eigenvalue. In another word, S belongs to span $\{\vec{1}\}$ when the corresponding graph is connected. That is, $M=\{S\in\Re^n|s_1=s_2=\cdots=s_n\}$.

Finally, we use LaSalle's invariance principle to concatenate the two previous convergence properties[36]. Let $\Omega=\Re^2$. The first and second step of the proof showed that every solution starting in Ω asymptotically converges to the invariant $\{\Omega_{path}\cap\Omega_u\}$. The third step showed that the largest invariant set of $\{\Omega_{path}\cap\Omega_u\}$, is the invariant manifold M. Therefore, every bounded solution starting in Ω converges to invariant manifold M which indeed is $s_1=s_2=\cdots=s_n$, as t tends to ∞.

Consequently, $u_d = U_{d0}\vec{1} - (\frac{u_{\max}-u_{\min}}{2\pi})\cdot\arctan(LS) = U_{d0}\vec{1} = (u_{i\max}+u_{i\min})/2$, which means each vehicle will always have the same velocity, to keep the same state value of s_i upon synchronizing the state S, so the vehicles will be synchronized to follow the predefined paths.∎

4 Examples

This section contains the results of simulation, illustrating the performance obtained by the control laws developed.

4.1 Case 1

Four homogenous underactuated AUVs with dynamics model of the INFANTE AUV[30], were required to follow 4 circumferences, which are with the same center but different radii R_i

$(i = 1, 2, 3, 4)$, respectively, while keeping synchronization with in-line formation.

The normalization of the along paths lengths for each underactuated AUVs is $\hat{s}_i = s_i/R_i$ and normalized speed is $\hat{u}_i = u_i/R_i$, will be the same in the case of circumferences. Actually, these normalized parameters make the truth, that the rotating speeds of virtual vehicles with respect to the same center of circles (i.e., angular frequencies), as well as normalized lengths along paths, are synchronized. Therefore, the in-line formation of multi-AUV systems is built.

The radius of the circumferences are $R = [5, 10, 15, 20]^{\mathrm{T}}$m. Four vehicles (scaled model) are with initial velocities of $u_0 = [2, 2, 2, 2]^{\mathrm{T}}$m/s, $v_0 = [0, 0, 0, 0]^{\mathrm{T}}$m/s, $r_0 = [0, 0, 0, 0]^{\mathrm{T}}$m/s. The maxim and minimum speed of the vehicles are $u^d_{\max} = 5.0$m/s and $u^d_{\min} = 0.1$m/s. The initial positions are $x = [0, 0, 0, 0]^{\mathrm{T}}$m and $y = [0, -5, -10, -15]^{\mathrm{T}}$m. The initial tracing error vectors are $s_{e0} = [5, 5, 5, 5]^{\mathrm{T}}$m and $y_{e0} = [5, 5, 5, 5]^{\mathrm{T}}$m. The initial error angles are $\psi_1 = [\pi/2, \pi/2, \pi/2, \pi/2]^{\mathrm{T}}$.

The Laplacian matrix, corresponding to the communication topology of the multi-AUV systems , is

$$L = D - A = \begin{pmatrix} 1 & -1 & 0 & 0 \\ -1 & 3 & -1 & -1 \\ 0 & -1 & 2 & -1 \\ 0 & -1 & -1 & 2 \end{pmatrix}.$$

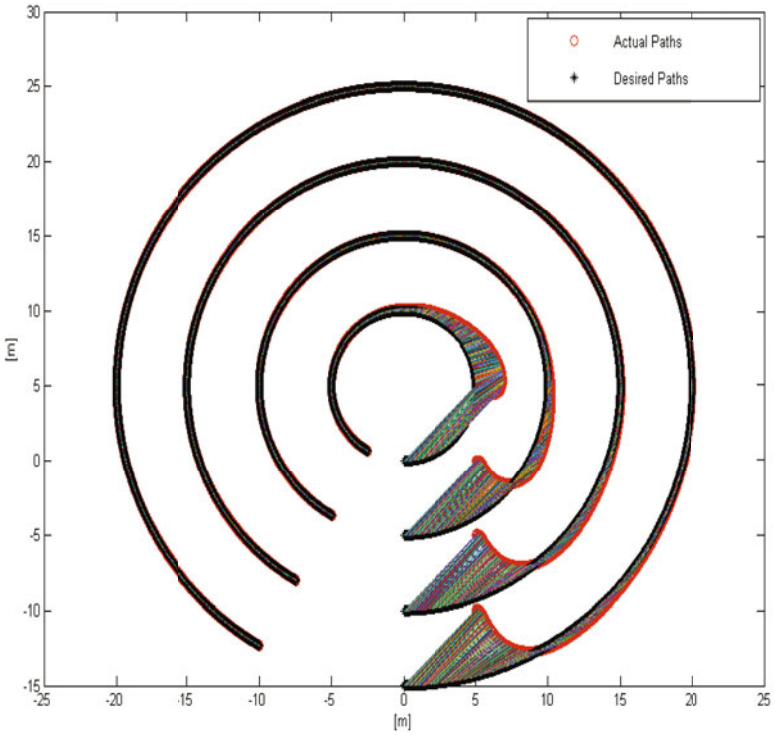

Figure 3 Synchronized in-line path following

As illustrated in Figure 3, the along path lengths of different vehicles converge to the same normalized value. The speed converges to the desired speed profile $U_d = [1, 2, 3, 4]^{\mathrm{T}}$m/s, as

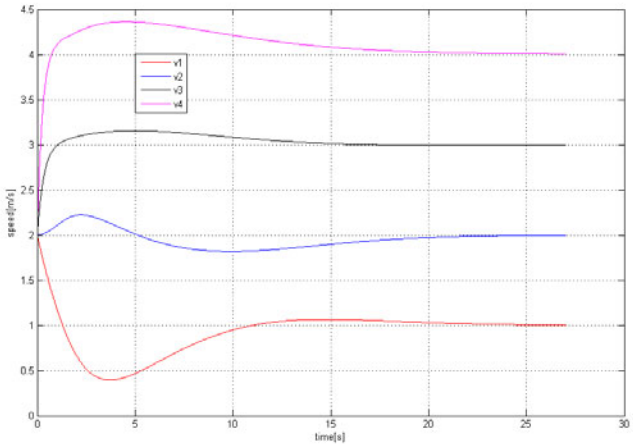

Figure 4 Synchronized speeds in in-line path following

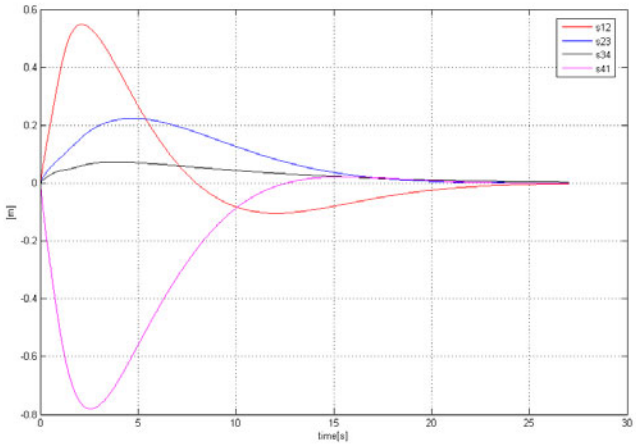

Figure 5 Normalized along path errors in path following

illustrated in Figure 4. The normalized synchronized errors s_{ij} $(= \hat{s}_i - \hat{s}_j)$ and u_{ij} $(= \hat{u}_i - \hat{u}_j)$ are illustrated in Figure 5 and 6, decaying to 0 respectively.

4.2 Case 2

Three homogenous underactuated AUVs with dynamics model of the INFANTE AUV, were required to inspect underwater pipeline. Therefore, AUVs follow three parallel curved paths based on the actual track of pipeline, while building varied geometric formation from "triangle" to "in-line", and then back to "triangle" formation. The parameterized paths are given as

$$x(\lambda) = \sum_{i=1}^{5} a_i \lambda^{i-1}, \quad y(\lambda) = \sum_{i=1}^{5} b_i \lambda^{i-1},$$

where $A = [a_i]^{\mathrm{T}} = [0, 0.87, -0.02, 10^{-5}, 1.5{\times}10^{-6}]^{\mathrm{T}}$; $B = [b_i]^{\mathrm{T}} = [0, 0.5, -5{\times}10^{-4}, 10^{-5}, 10^{-7}]^{\mathrm{T}}$.

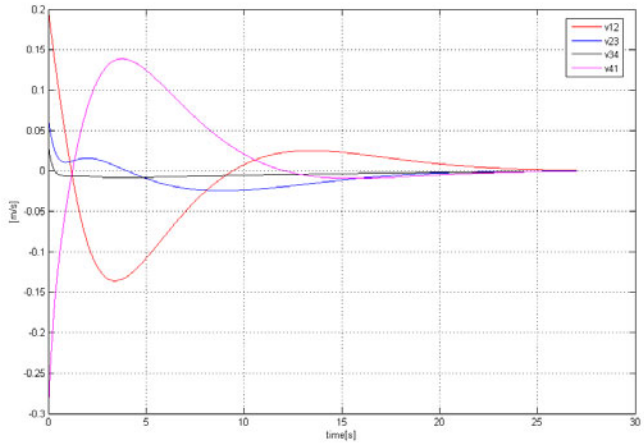

Figure 6 Normalized speed errors in path following

The initial position of three AUVs are $x = [30, 20, 40]^{\mathrm{T}}\mathrm{m}$ and $y = [-30, -30, -30]^{\mathrm{T}}\mathrm{m}$. The initial velocities of $u_0 = [0.1, 0.1, 0.1]^{\mathrm{T}}\mathrm{m/s}, v_0 = [0, 0, 0]^{\mathrm{T}}\mathrm{m/s}, r_0 = [0, 0, 0]^{\mathrm{T}}\mathrm{m/s}$, and the initial orientation are $\psi_1 = [\pi/2, \pi/2, \pi/2]^{\mathrm{T}}$. The communication topology is

$$L = D - A = \begin{pmatrix} 1 & -1 & 0 \\ -1 & 2 & -1 \\ 0 & -1 & 1 \end{pmatrix}.$$

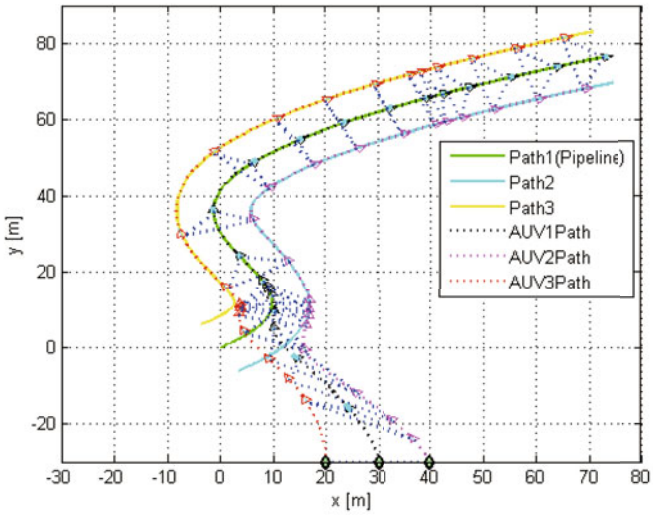

Figure 7 Synchronized path following in varied formation topology

For the "triangle formation", the along-path distance between the "tip" AUV and other two "bottom" AUVs is 5m. This along-path distance in "triangle" can be introduced as an offset of the normalized parameters $\hat{s}_i$, such that the same synchronized path following control law can

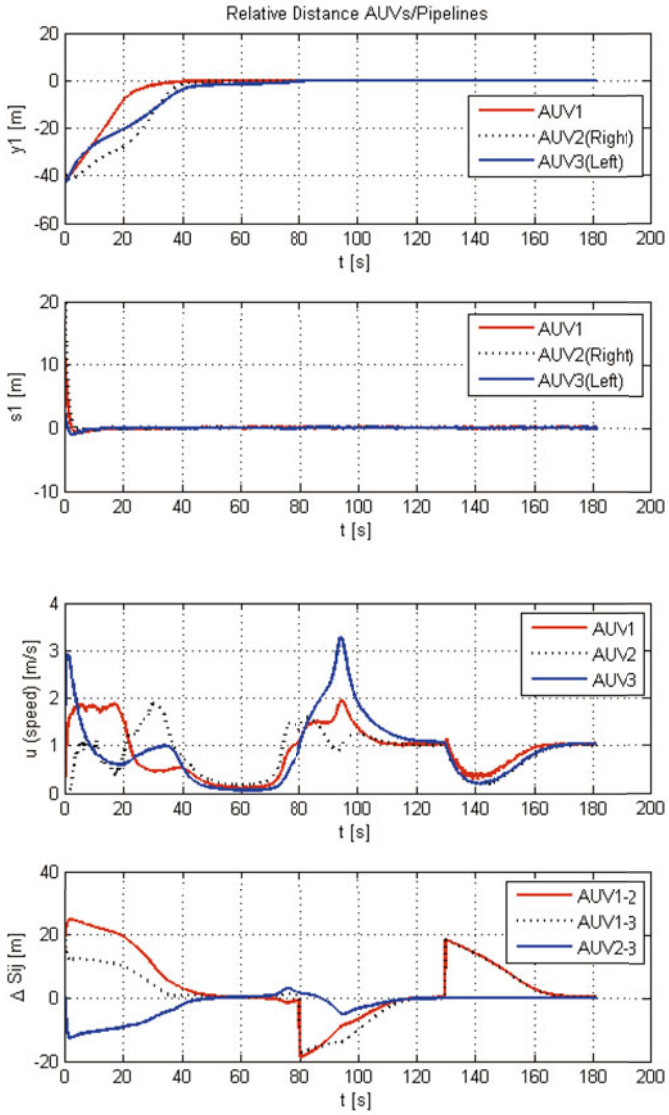

Figure 8 AUVs speeds and synchronized errors

be utilized. As illustrated in Figure 7, the "triangle-inline-triangle" formation along the desired path has been well built via synchronized control. The tracking error for each AUV is shown in Figure 8, where the along-track error and cross-track error converges to 0. The top figure in Figure 8 shows the speed profile of AUVs converging to the desired speed $u_d = 1\text{m/s}$, and the bottom figure in Figure 8 clearly shows the distances between each pair of AUVs, coinciding with the procedure during building "triangle-inline-triangle" formation.

5 Conclusions

The paper addresses the problem of synchronized path following of multiple vehicles. There

are two-layer controllers for each vehicle in the team, decoupled in geometric task and synchronization task. One is the individual path following controller, which drives the vehicle converging to the paths, with a helmsman-like behavior embedded in heading reference design. The other is the controller for synchronization in global sense, which is realized by means of decentralized speed adaptation. The minimum communication variables is requested here, and the communication topology is not necessarily all-to-all. A formal proof of convergence for each (individual/synchronized path following) controller is derived in detail, and simulations illustrated the efficacy of the solution proposed.

Further work will address the case where vehicles are required to follow generalized spatial paths in synchronization, the time-delay in acoustic link and switched topology of communication network is also of interest. Additional attentions should also be paid to simultaneously path following and obstacle avoidance/collision free of multi-AUV systems , in order to guarantee motion safety for each autonomous vehicle.

References

[1] R. Beard, J. Lawton, and F. Hadaegh, A coordination architecture for spacecraft formation control. *IEEE Transactions on Control Systems Technology*, 1999, **9**(6): 777–790.

[2] I. Kaminer, O. Yakimenko, A. Pascoal, and R. Ghabcheloo, Path generation, path following and coordinated control for time critical missions of multiple UAVs. *Proceeding of the IEEE American Control Conference, Minneapolis, MN*, 14–16 June, 2006.

[3] J. Desai, J. Otrowski, and V. Kumar, Controlling formations of multiple robots, *Proceeding of the IEEE International Conference on Robotics and Automation* (*ICRA*98)*, Leuven, Belgium*, 16–20 May, 1998.

[4] P. Ogren, E. Fiorelli, and N. E. Leonard, Cooperative control of mobile sensor networks: Adaptive gradient climbing in a distributed environment, *IEEE Transactions on Automatic Control*, 2004, **49**(8): 1292–1302.

[5] N. E. Leonard and E. Fiorelli, Virtual leaders, artificial potentials and coordinated control of groups, *Proceeding of the IEEE Control and Decision Conference, Orlando, FL*, 2001.

[6] F. Zhang, D. M. Fratantoni, D. Paley, J. Lund, and N. E. Leonard, Control of coordinated patterns for ocean sampling, *International Journal of Control*, 2007, **80**(7): 1186–1199.

[7] R. M. Murray, Recent research in cooperative control of multi-vehicle systems, *ASME Journal of Dynamic Systems, Measurement and Control*, 2006, **129**(5): 571–583.

[8] K. Y. Wichlund, O. J. Sordalen, and O. Egeland, Control of vehicles with second-order nonholonomic constraints: Underactuated vehicles, *Proceedings of the European Control Conference, Rome, Italy*, Sep., 1995.

[9] A. M. Bloch, J. Baillieul, P. Crouch, and J. Marsden, *Nonholonomic Mechanics and Control,* Springer-Verlag, New York, 2003.

[10] R. Murray and S. Sastry, Nonholonomic motion planning: Steering using sinusoids, *IEEE Transactions on Automatic Control*, 1993, **38**(5): 700–716.

[11] Z. P. Jiang, Iterative design of time-varying stabilizers for multi-input systems in chained form, *Systems Control Letters*, 1996, **28**(5): 255–262.

[12] I. F. Akyildiz, D. Pompili, and T. Melodia, Underwater acoustic sensor networks: Research challenges, *Ad Hoc Networks*, 2005, **3**(3): 257–279.

[13] D. Schoenwald, AUVs: In space, air, water, and on the ground, *IEEE Control Systems Magazine*, 2000, **20**(6): 15–18.

[14] P. Encarnacao and A. Pascoal, 3D path following for autonomous underwater vehicle, *Proceedings of the* 39*th IEEE Conference on Decision and Control, Sydney, Australia*, 12–15, Dec., 2000.

[15] L. Lapierre, D. Soetanto, and A. Pascoal, Coordinated motion control of marine robots, *Proceedings of the* 6*th IFAC Conference on Manoeuvering and Control of Marine Craft, Girona, Spain*, 2003.

[16] D. Stilwell and B. Bishop. Platoons of underwater vehicles, *IEEE Control System Magazine*, 2000, **20**(6): 45–52.
[17] A. Fax and R. Murray, Graph Laplacians and stabilization of vehicle formations, *IEEE Transactions on Automatic Control*, 2004, **49**(9): 1465–1476.
[18] R. O. Saber and R. M. Murray, Consensus problems in networks of agents with switching topology and time-delays, *IEEE Transactions on Automatic Control*, 2004, **49**(9): 1520–1533.
[19] L. Moreau, Stability of multiagent systems with time-dependent communication links, *IEEE Transactions on Automatic Control*, 2005, **50**(2): 169–182.
[20] W. Ren and R. W. Beard, Consensus seeking in multiagent systems under dynamically changing interaction topologies, *IEEE Transactions on Automatic Control*, 2005, **50**(5): 655–661.
[21] R. Olfati-Saber, Flocking for multi-agent dynamic systems: Algorithms and theory, *IEEE Transactions on Automatic Control*, 2006, **51**(3): 401–420.
[22] Craig W. Reynolds, Flocks, herds and schools: A distributed behavioral model, *Proceedings of the 14th Annual Conference on Computer Graphics and Interactive Techniques*, New York, NY, USA, 1987.
[23] A. Jadbabaie, J. Lin, A. S. Morse, Coordination of groups of mobile autonomous agents using nearest neighbor rules, *IEEE Transactions on Automatic Control*, 2003, **48**(6): 988–1001.
[24] R. Ghabcheloo, A. Pascoal, C. Silvestre, and I. Kaminer, Coordinated path following control of multiple wheeled robots using linearization techniques, *International Journal of Systems Science*, 2005, **37**(6): 399–414.
[25] R. Ghabcheloo, A. Pascoal, C. Silvestre and I. Kaminer, Nonlinear coordinated path following control with bidirectional communication constraints, *Group Coordination and Cooperative Control, Springer Series on Lecture Notes in Control and Information Sciences*, 2006.
[26] R. Skjetne, S. Moi, and T. Fossen, Nonlinear formation control of marine craft, *Proceedings of the IEEE Conference on Decision and Control, Las Vegas, NV.*, 2002.
[27] L. Lapierre, D. Soetanto and A. Pascoal, Nonlinear path following with applications to the control of autonomous underwater vehicles, *Proceedings of the IEEE Conference on Decision Control, Maui, Hawaii*, Dec. 9–12, 2003.
[28] C. Samson, Path following and time-varying feedback stabilization of a wheeled mobile robot, *Proceedings of the International Conference on Advanced Robotics and Computer Vision, Singapore*, 1992, **13**(1): 1–5.
[29] M. Egerstedt, X. Hu, and A. Stotsky, Control of mobile platforms using a virtual vehicle approach, *IEEE Transactionon Automatic Control*, 2001, **46**(11): 1777–1782.
[30] C. Silvestre, Multi-objective optimization theory with application to the integrated design of controllers/plants for autonomous vehicle, Ph.D. dissertation, Robot. Dept., Instituto Superior Tecnico (IST), Lisbon, Portugal, Jun. 2000.
[31] T. Fossen, *Guidance and Control of Ocean Vehicles*, Wiley, New York, 1994.
[32] T. Fossen, M. Breivik, and R. Skjeme, Line-of-sight path following of underactuated marine craft, *Proceedings of the 6th IFAC Conference on Manoeuvering and Control of Marine Craft, Girona, Spain*, 2003.
[33] M. Krstic, I. Kanellakopoulos, and P. Kokotovic *Nonlinear and Adaptive Control Design*, John Willey & Sons Inc., New York, 1995.
[34] L. Lapierre and B. Jouvencel, Robust nonlinear path-following control of an AUV, *IEEE Journal of Oceanic Engineering*, 2008, **33**(2): 89–102.
[35] C. Godsil and G. Royle, *Algebraic Graph Theory, Graduated Texts in Mathematics*, Springer-Verlag, New York, 2001.
[36] H. K. Khalil, *Nonlinear Systems*, Prentice-Hall, Upper Saddle River, NJ, 1996.